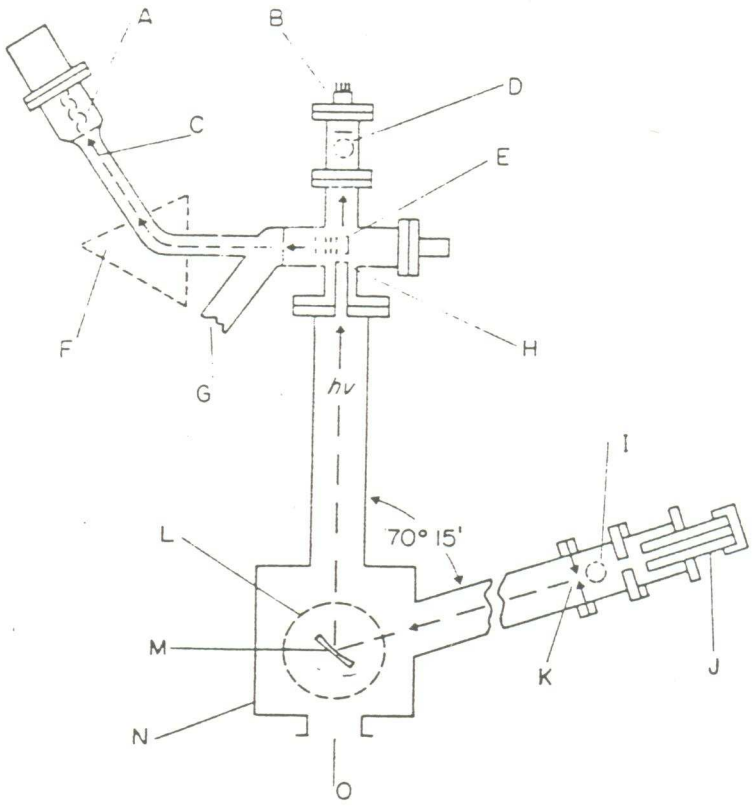

. 2. Vacuum monochromator and mass spectrometer. A, electron multiplier ion detector; B, photomultiplier radiation
ion beam; D, G, I, O, to pumping systems; E, ion chamber; F, permanent magnet; H, monochromator exit slit; J, light
monochromator entrance slit; L, grating turntable; M, grating; N, Seya type vacuum monochromator (Weissler et al. [

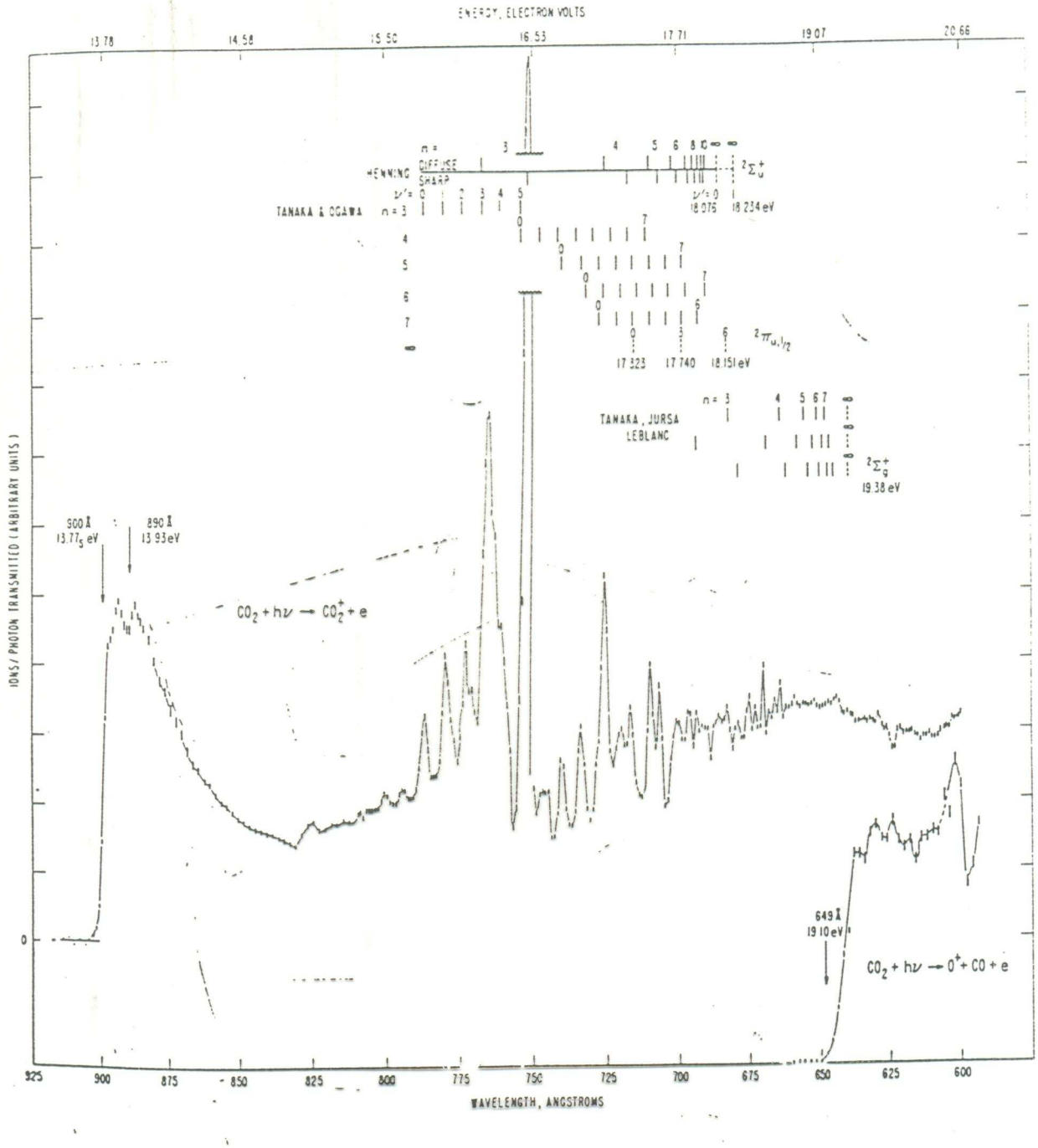

. 18. Photoionization-efficiency curves for the CO_2^+ and O^+ ions of carbon dioxide. The ordinate scale for the molecule ion is 20 es that of the atom ion (Dibeler and Walker [111]).

UPS

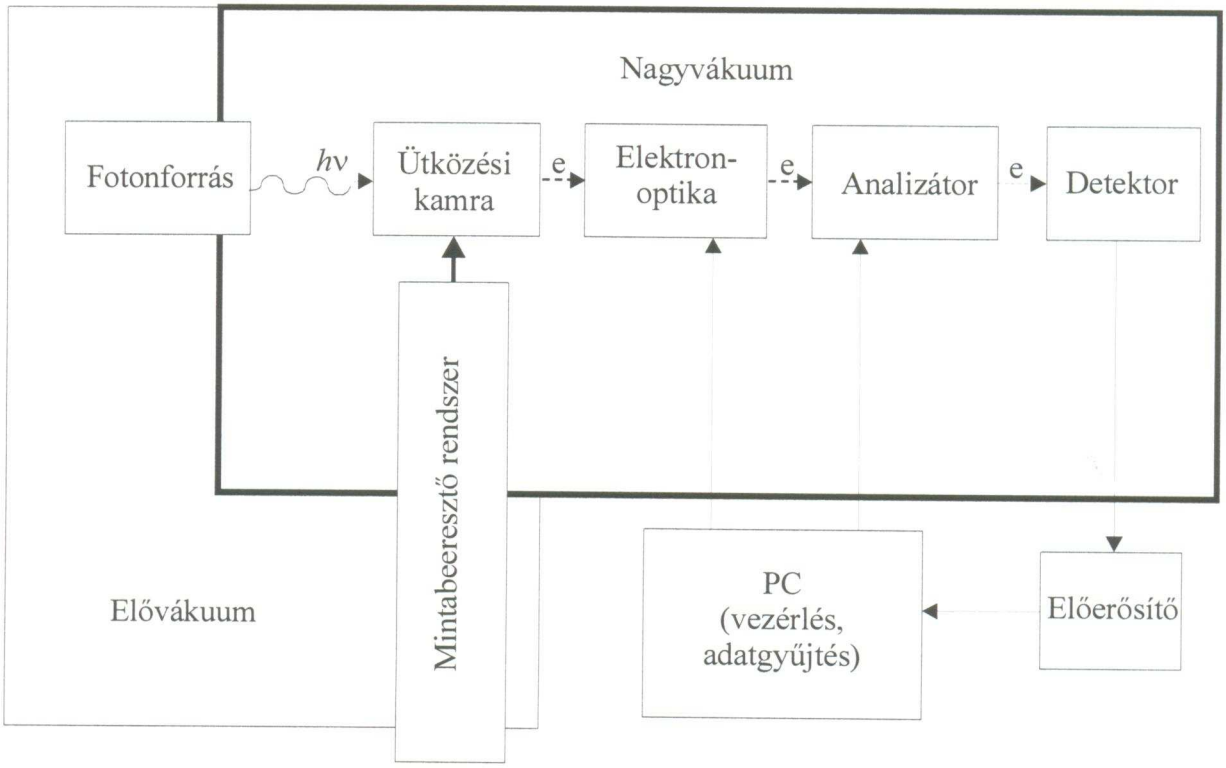
Nagyvákuum
Fotonforrás
hν
Ütközési kamra
e
Elektron-optika
e
Analizátor
e
Detektor
Mintabeeresztő rendszer
Elővákuum
PC (vezérlés, adatgyűjtés)
Előerősítő

PEPICO

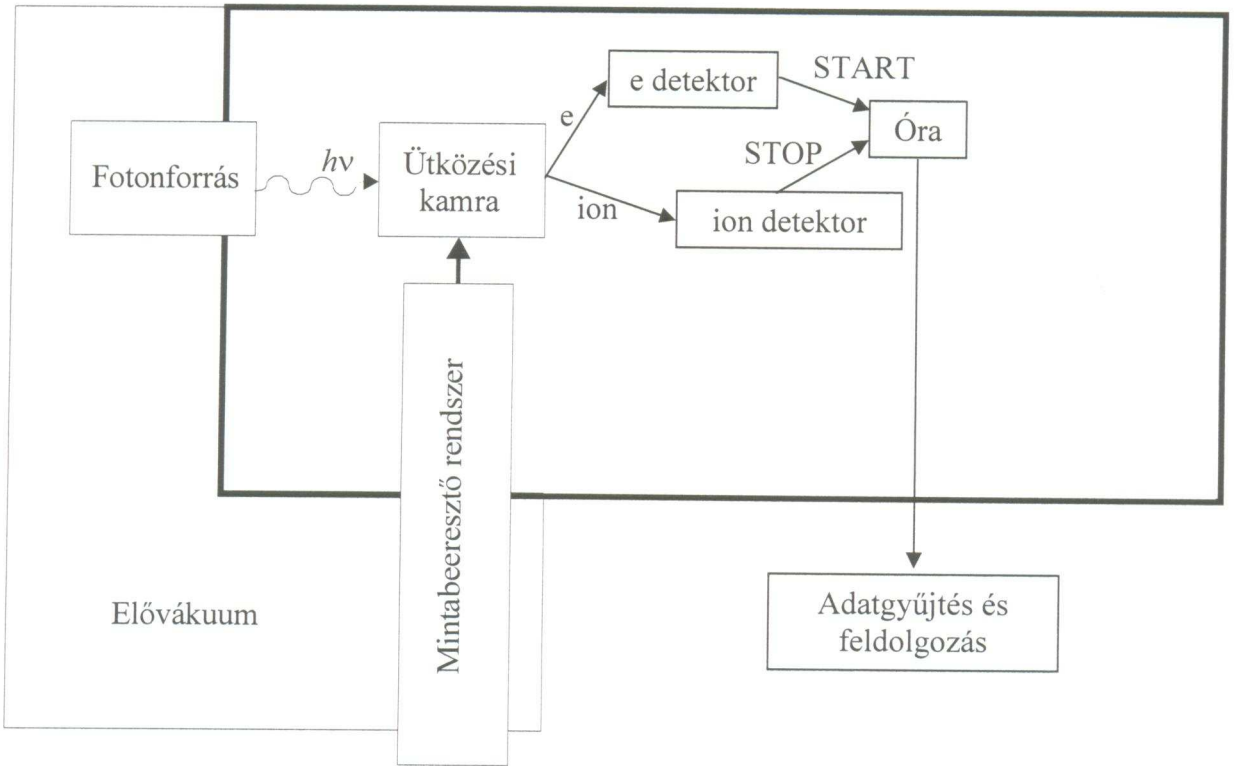
e detektor
START
Óra
e
STOP
Fotonforrás
hν
Ütközési kamra
ion
ion detektor
Mintabeeresztő rendszer
Elővákuum
Adatgyűjtés és feldolgozás

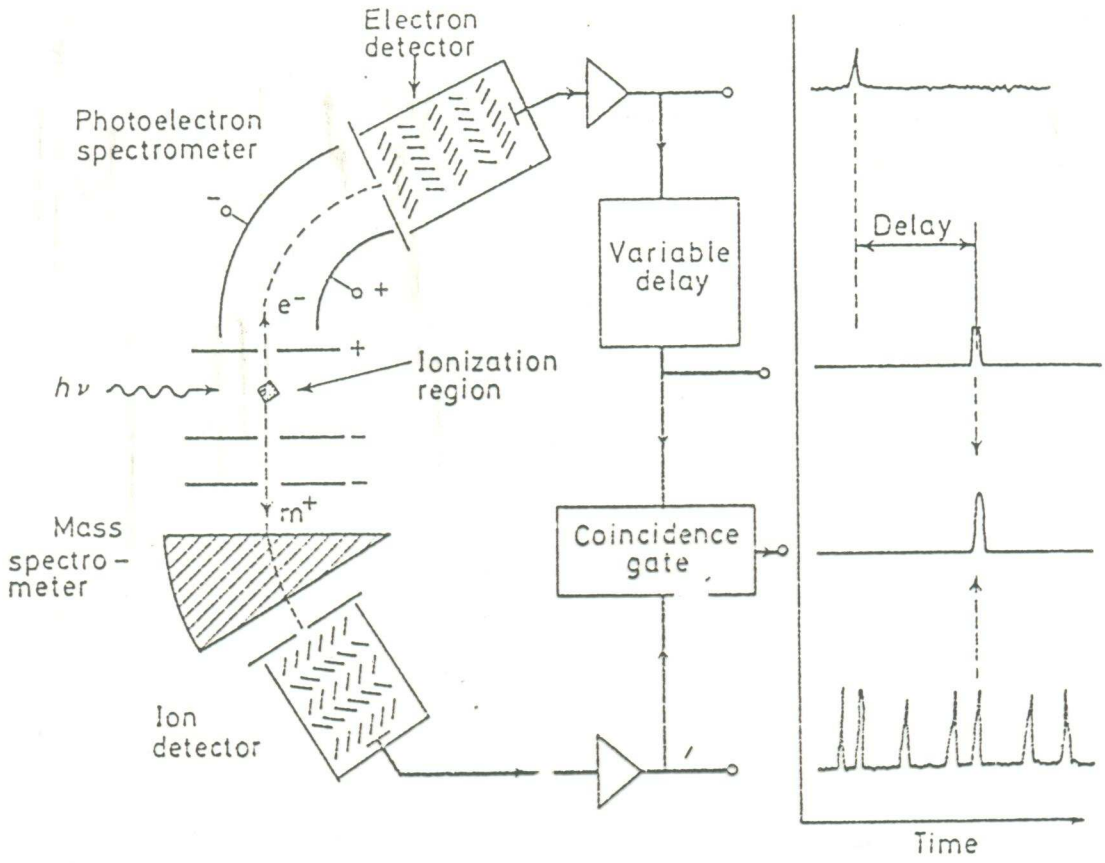

Figure 7.5. Simplified scheme of a photoelectron–photoion coincidence spectrometer. The peaks in the idealized wave-forms on the right indicate detection of single electrons and single ions; there are generally many more ions than electrons because the collection efficiency of mass spectrometers is higher than that of photoelectron spectrometers

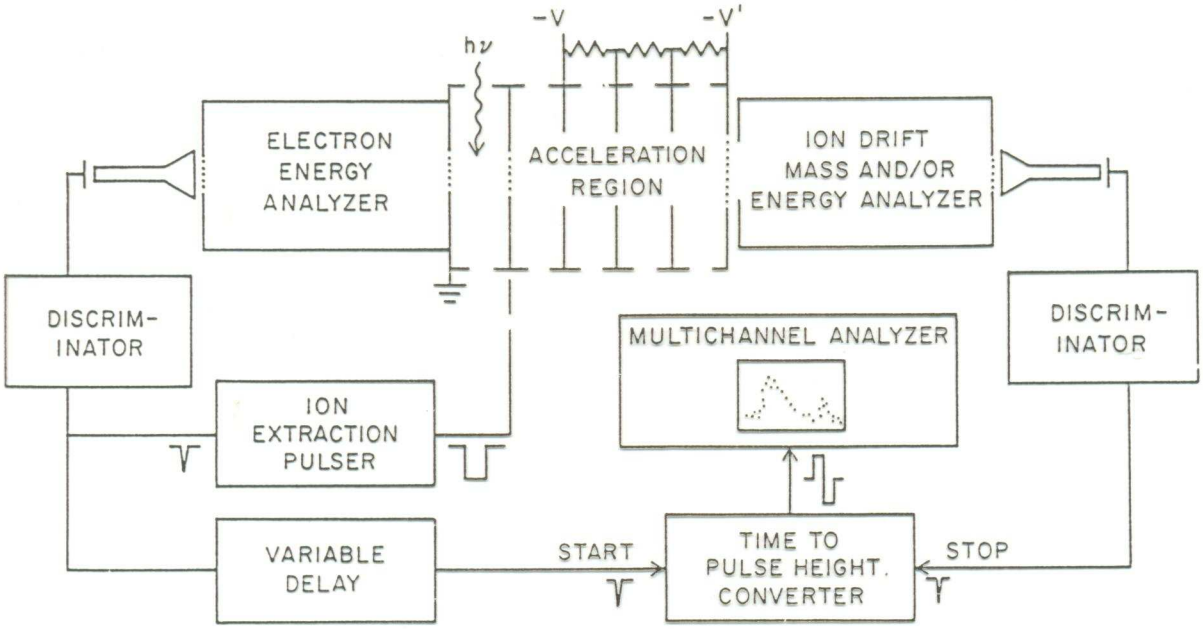

FIG. 1 Block diagram of a photoion–photoelectron coincidence experiment.

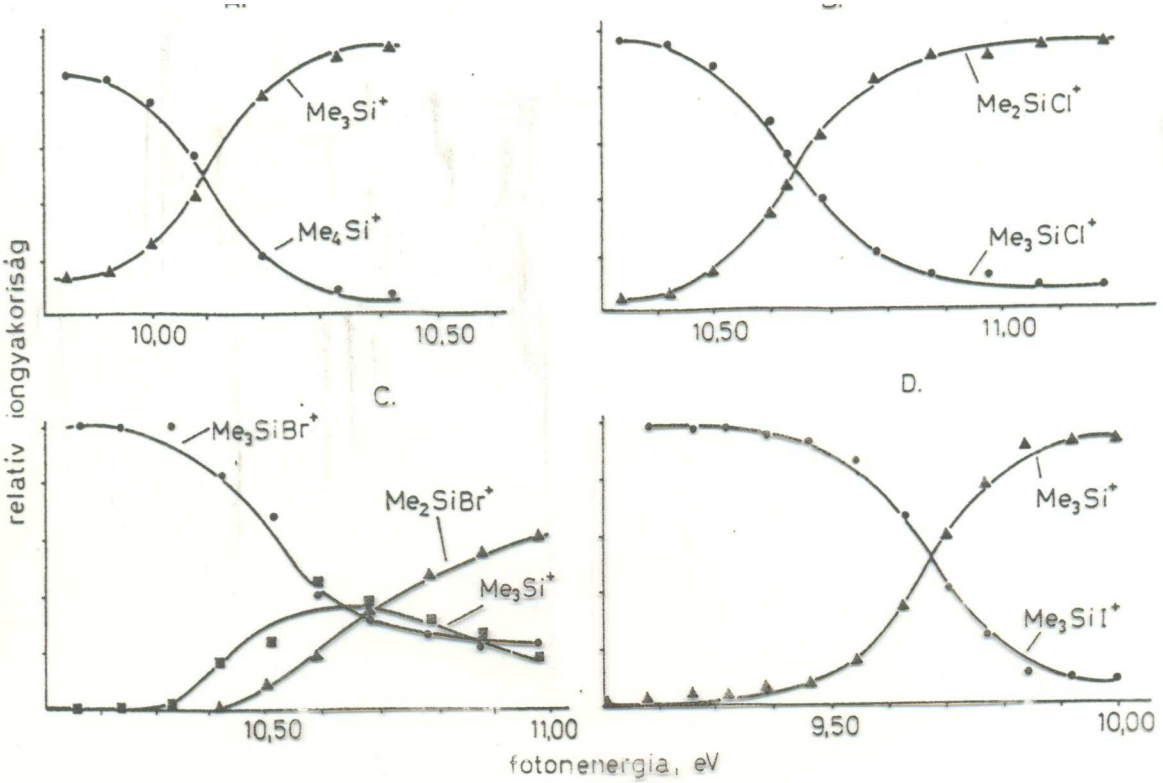

2. ábra

A tetrametil-, trimetil-klór-, trimetil-bróm- és trimetil-jód-szilán letörési diagramja

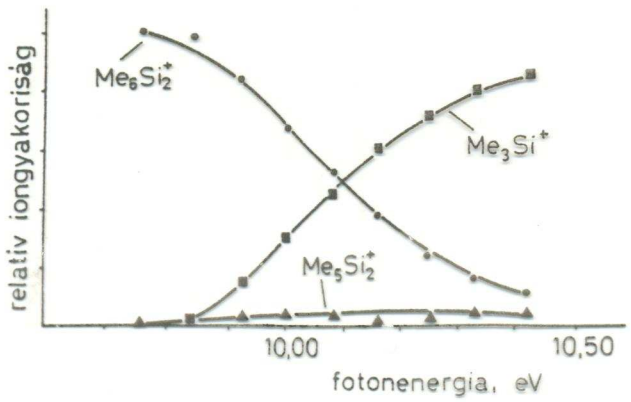

1. ábra

A hexametil-diszilán letörési diagramja

MG-12.

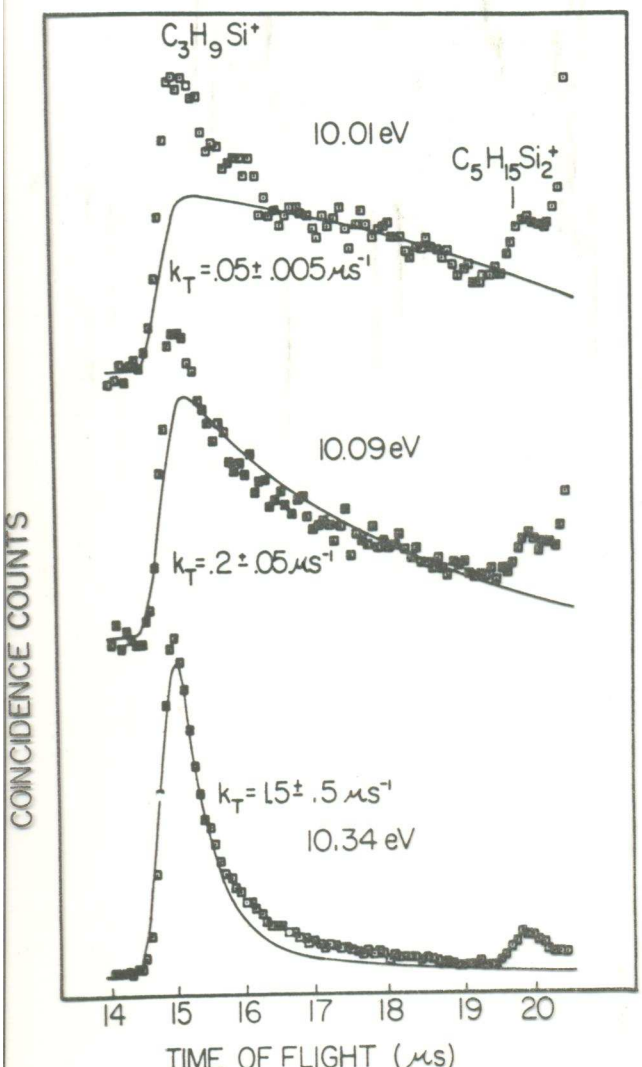

e 3. Time-of-flight (TOF) spectra for Me_3Si^+ (m/z 73) and i_2^+ (m/z 131) at three different photon energies in the metastable y region.

butions in coincidence with zero kinetic energy electrons, over ion of ion internal energies ranging from 9.9 to 11.0 eV. Some e results are shown in Figure 3, in which the points are the rimental data while the solid curves are calculated TOF ibution based on a single unimolecular decay. The experi- tal TOF distributions at the lower energies clearly exhibit a peak on top of the very asymmetric Me_3Si^+ peak. This peak tually extremely weak but shows up at low photon energies hich the slow $HMDS^+$ dissociation produces a very weak m/z eak. For the reasons outline below, this sharp peak is at- ıted to an impurity. A mass spectrum at 9.6 eV, well below energy at which the m/z 73 peak is apparent, showed two s at m/z 72 and 104. The higher mass peak was eliminated purification by GLC. However, this procedure did not ıge the amount of the m/z 72 component. Because this peak mmetric, it can only come from a molecular ion (i.e., im- ty), or from a rapid dissociation of the HMDS parent ion. latter would imply a nonstatistical dissociation, an explanation ch is not likely and is not supported by any other findings of study. We therefore conclude that it arises from an impurity, ch is present in minute amounts. Nevertheless, it is evident result of the long counting times required near the $HMDS^+$ ociation threshold.

he experimentally determined rates in Figure 3 are total rates

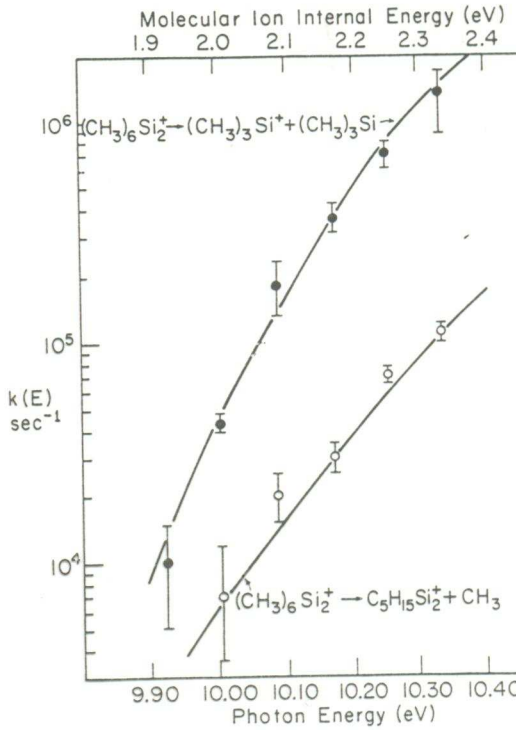

Figure 4. The decay rate, $k(E)$, as a function energy for t of hexamethyldisilane$^+$ to Me_3Si^+ + $Me_3Si\cdot$ and Me_5Si_2 solid curves are the results of RRKM/QET calculation brational frequencies of Table III and activation energies o eV respectively for the production of m/z 73 and 131. T (ion internal energy) is related to the photon energy b ionization energy minus the HMDS internal thermal en 300 K is 0.260 eV.

When different products originate from the sar the total decay rates can be converted into rates of the individual fragments by using the ratios of t area as ratios of rates to various fragments. This been discussed and applied previously.[18,28] The res in Figure 4 where the points are the experimentall rate constants at different photon energies. The $k(E$ of Me_3Si^+ formation rises more rapidly with a rise i that of the $Me_5Si_2^+$ ion. In terms of RRKM/QE a tighter activated state for $Me_5Si_2^+$ formation. On t by extrapolating to lower energies one can expect a resulting in a lower thermochemical threshold fo

According to the statistical theory[29,30] (RRK unimolecular decay rate is given by

$$k(E) = \sigma \frac{\int_{\epsilon=0}^{E-E_0} \rho^\ddagger(E)\, d\epsilon}{h\rho(E)}$$

where E_0 is the minimum energy needed for reac are the densities of internal energy for the transi precursor ions, respectively, and σ is a statistical f the number of independent ways the transition state For $k(E)$ to be calculated, E_0 and vibrational frequ transition state and molecular ion must be assum reactions the vibrational frequencies for the molec assumed to be those of the neutral molecule.[31,32] By combinations of the other two parameters, best fits lines in Figure 4 were found. The best transition-sta for production of m/z 73 and 131 ions together with ion normal vibrations are listed in Table III. In

RRKM/QET

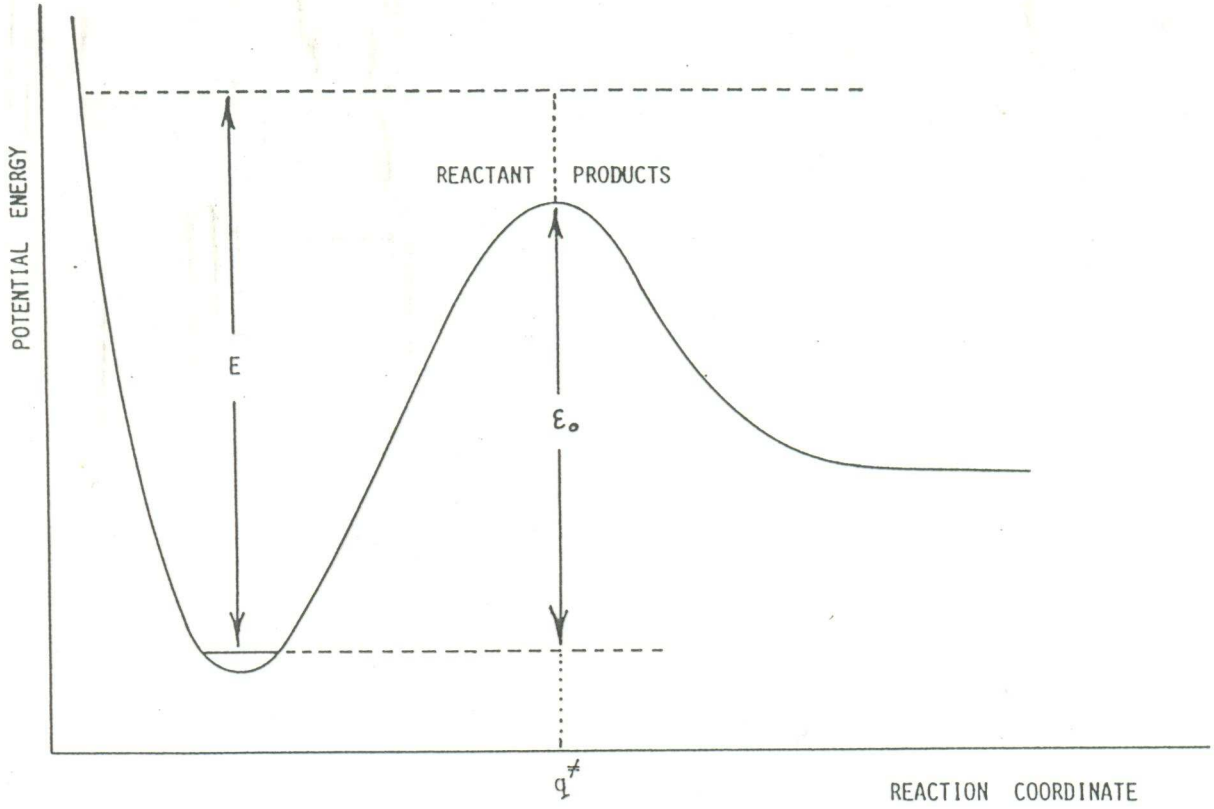

$$k(E) = \sigma \frac{\int_{\epsilon=0}^{E-E_0} \rho^{\ddagger}(E)\, \mathrm{d}\epsilon}{h\rho(E)}$$

$$k(E) = \frac{\prod^{s} \nu_i}{\prod^{s-1} \nu_i^{\neq}} \left(\frac{E - \varepsilon_0}{E} \right)^{s-1}$$

$$k(E) = \frac{\prod^{s} \nu_i}{\prod^{s-1} \nu_i^{\neq}} \left(\frac{E - \varepsilon_0 + E_z^{\neq}}{E + E_z} \right)^{s-1}$$